Journal of
Materials Chemistry A

Materials for energy and sustainability

Accepted Manuscript

This article can be cited before page numbers have been issued, to do this please use: F. Ebadi, B. Yang, Y. Kim, R. Mohammadpour, N. Taghavinia, A. Hagfeldt and W. Tress, *J. Mater. Chem. A*, 2021, DOI: 10.1039/D1TA02878B.

ROYAL SOCIETY OF CHEMISTRY

rsc.li/materials-a

View Article Online
DOI: 10.1039/D1TA02878B

When photoluminescence, electroluminescence, and open-circuit voltage diverge – light soaking and halide segregation in perovskite solar cells

*Firouzeh Ebadi[1e], Bowen Yang[2e], YeonJu Kim[2], Raheleh Mohammadpour[3], Nima Taghavinia[3,4], Anders Hagfeldt[2], Wolfgang Tress,[1,2]**

[1]Institute of Computational Physics, Zurich University of Applied Sciences, Wildbachstr. 21, 8401 Winterthur, Switzerland

[2]École Polytechnique Fédérale de Lausanne, Laboratory of Photomolecular Science, 1015 Lausanne, Switzerland.

[3]Institute for Nanoscience and Nanotechnology, Sharif University of Technology, Tehran 14588, Iran.

[4]Department of Physics, Sharif University of Technology, Tehran 14588, Iran.

[e]contributed equally

ABSTRACT

Perovskite solar cells suffer from various instabilities on all time scales. Some of them are driven by light, in particular when employing compounds with mixed halides. Such light soaking effects have been observed in performance changes of solar-cell devices. They have also been spectroscopically investigated in detail on films, where the formation of a low-gap iodine rich phase, seen in a red shift of the PL has been made responsible for a reduced open-circuit voltage. However, studies synchronously examining device performance and its relation to spectroscopy data, are scarce. Here, we perform an *in-operandum* study, where we investigate changes of open-circuit voltage (V_{oc}) and photocurrent during light soaking and complement it with photo- (PL) and electroluminescence (EL) data on devices, which allow analysis of the V_{oc}-limiting processes using optical and optoelectronic reciprocity relations. We find that changes in the V_{oc} for stable single halide compositions are quantitatively correlated with changes in the PL intensity, showing that the V_{oc} follows changes in the quasi-Fermi level splitting. In contrast, changes in V_{oc} for the mixed halide composition are not correlated to the emergence of the low-gap phase, confirming that this phase is not the sole culprit for a low and instable V_{oc}. Instead, non-radiative voltage losses influenced by mobile ions are dominant in devices containing compositions with high Br content. Interestingly, the low-gap phase contributes less to photocurrent, as seen by a wavelength-dependent PL quenching at short circuit. This observation might be explained by the formation of emissive but partially insulated iodine-rich regions in the film. Such an effect is also possible for single halide systems, when the perovskite composition is not stable, seen in an increase of PL at short circuit during light soaking. This indicates that ion migration in general causes photovoltaically inactive regions, without enhancing non-radiative recombination, an effect that might need to be considered in the analysis of PL quantum yields. EL measurements confirm that Rau's reciprocity relation between external EL quantum efficiency and V_{oc} cannot readily be applied to absorbers with such different phases.

Introduction

To reach the ultimate (i.e. thermodynamic) performance limit of a solar cell, recombination processes have to be solely radiative. For an abrupt absorption onset at the bandgap energy, this radiative limit is the well-known Shockley-Queisser limit.[1] In such a situation the open-circuit voltage (V_{oc}) is

View Article Online
DOI: 10.1039/D1TA02878B

optimum. Any additional non-radiative recombination causes a reduction of charge carrier densities and therefore the V_{oc}. Hence, there is a correlation between luminescence yields and V_{oc} – the higher the yield, the higher V_{oc}.[2] This fundamental correlation has also been observed for perovskite solar cells in various studies.[3] It can either be measured in terms of electroluminescence, where the solar cell is driven as an LED[4] or in photoluminescence.[5,6] The latter has the advantage of being a non-contact measurement, allowing for a determination of the chemical potential of electrons and holes (quasi-Fermi level splitting) also in films. Thus, the potential of a material regarding V_{oc} can be estimated before a device has been fabricated and additional recombination induced by the contact materials can be identified.[5–7]

In this study we simultaneously measure the evolution of the luminescence (PL and EL) and solar cell parameters during light soaking to gain insights into loss processes in perovskite solar cells with and without halide segregation. Despite of various studies on reversible halide segregation[8] including effects such as a narrow temperature window,[9] a dependence on composition,[10] grain size[11] and the grain topography affecting mainly regions close to grain boundaries,[12] suppression by nano crystals,[13] a pressure dependent remixing[14] and discussions on irreversible changes,[15] its effect on the device performance is only rudimentarily investigated. Commonly, general claims are made that phase segregation blocks the charge carrier flux and induces recombination.[16] In a recent study a correlation of red-shifted PL and reduced open-circuit voltage (only under high light intensity) has been observed.[17] A very recent study addresses PL on devices during light soaking with hypotheses on a complex interaction of different types of defect species and grain-boundary mediated charge transport.[18] Beyond the bulk of the film, surfaces have been found to influence phase segregation,[19] indicating that observations on films are not necessarily sufficient to describe effects on the device.

We observe that the correlation of PL or EL yield and open-circuit voltage does not hold during light soaking in generally instable systems regardless of the formation of a low-gap phase. We explain this by the formation of though emissive but insulated regions in the perovskite that contribute less to photocurrent. The formation of such regions is obvious for the systems with phase segregation, where not only the yield increases but also the peak wavelength shifts. However, this effect is not limited to the mixed halide systems meaning that the low-gap phase upon halide phase segregation by itself is not the sole cause for a reduced performance of our devices during light soaking. Instead, in both cases photocurrent and photovoltage losses follow a common scheme.

Results

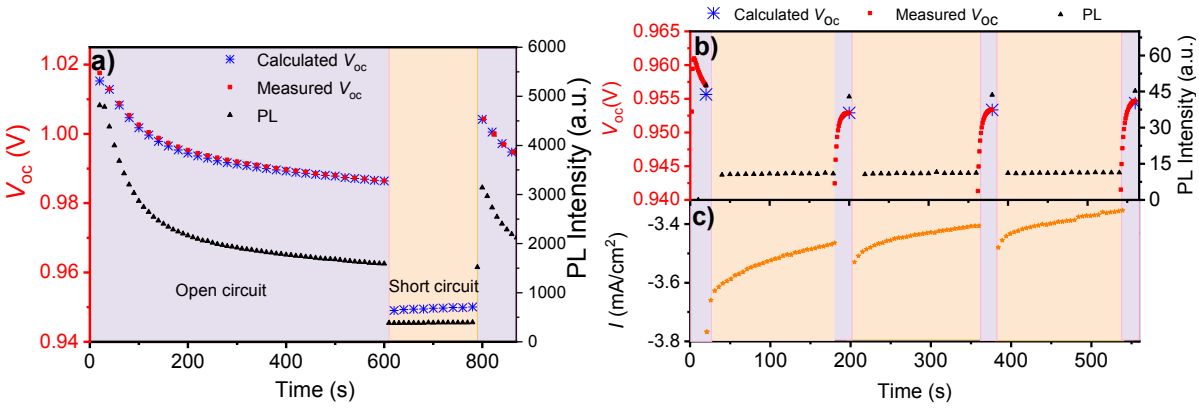

Figure 1. Evolution of open-circuit voltage (V_{oc}) and PL intensity during light soaking of a device containing $CsFAPbI_3$. (a) Predominantly under open circuit (b) mainly under short circuit. (c)

View Article Online
DOI: 10.1039/D1TA02878B

Corresponding current density under short circuit. In both cases (a,b), the calculated V_{oc} based on the change of the PL intensity matches the measured V_{oc}.

For best comparability and to exclude halide phase segregation of our reference device, we chose perovskite of the nominal composition $Cs_{0.1}FA_{0.9}PbI_3$ to be compared with $Cs_{0.1}FA_{0.9}Pb(I_{0.65}Br_{0.35})_3$. Although mixed-cation mixed-halide compositions (with low Br content) have been proven to be more stable,[20] reversible composition changes upon illumination have been observed such as enrichment of Br close to the surface,[21] which can be suppressed by addition of Cs.[22] Other studies report I enrichement[23] – for higher Br ratios also in combination with the formation of PbI_2 at the surface.[24] We emphasize that our study is on in-operando PL spectra and device performance during light-driven reversible halide segregation, which is a very intrinsic property. We do not study phase segregation in general or induced by other factors such as humidity.[25] Our perovskite layer, whose morphology is comparable for the two compositions (Fig. SI1), is sandwiched between mesoporous TiO_2 and doped spiro-MeOTAD/Au (details in experimental section in Table SI1). Light soaking is performed under monochromatic blue laser light (422 nm), that illuminates the sample homogeneously through a diffuser plate resulting in light intensities in the order of 30% of a sun, which represent realistic solar operation conditions. PL spectra are recorded with a spectrometer equipped with a CCD camera (details in the experimental section).

Figure 1a shows the development of V_{oc} upon turning on the illumination. V_{oc} decreases during keeping the device at open circuit and partially recovers after a period (from 600 to 800 s) under short circuit, confirming the interplay between light and voltage effects on the results and excluding a dominant temperature influence (heating). This trend has widely been observed, in particular for n-i-p architecture devices.[26] Here, we add the simultaneously monitored evolution of the PL (black) and calculate a predicted V_{oc} (blue) based on the change of the PL intensity: $V_{\mathrm{oc}}(t) - V_{\mathrm{oc},0} = \frac{kT}{e}\ln\frac{I_{\mathrm{PL}}(t)}{I_{\mathrm{PL},0}}$. The calculated V_{oc} perfectly follows the measured one, being consistent with the theory outlined in the introduction. In a control experiment, we measure the evolution of PL of a film, which remains roughly constant (Fig. SI2a), confirming that the decrease of PL and V_{oc} is related to changes of non-radiative recombination at the contacts as already previously discussed.[27] During light soaking, we do not observe deviations between PL yield and V_{oc}, which could occur in case of surface-recombination induced high gradients in the quasi-Fermi levels,[28,29] as recently reported for perovskite devices with a poor hole transport layer.[7] Commonly, other compositions such as $MAPbI_3$ and devices with low Br content behave more or less in the same way (Fig. SI3-6), excluding that the mixed monovalent cations of our single-halide device play a crucial role.[30] This observation holds for light-soaking under short circuit as well, where the V_{oc} (probed every 3 minutes) decrease is much less pronounced, but the PL can still be used to quantify the changes of V_{oc} (**Fig. 1b**).

View Article Online
DOI: 10.1039/D1TA02878B

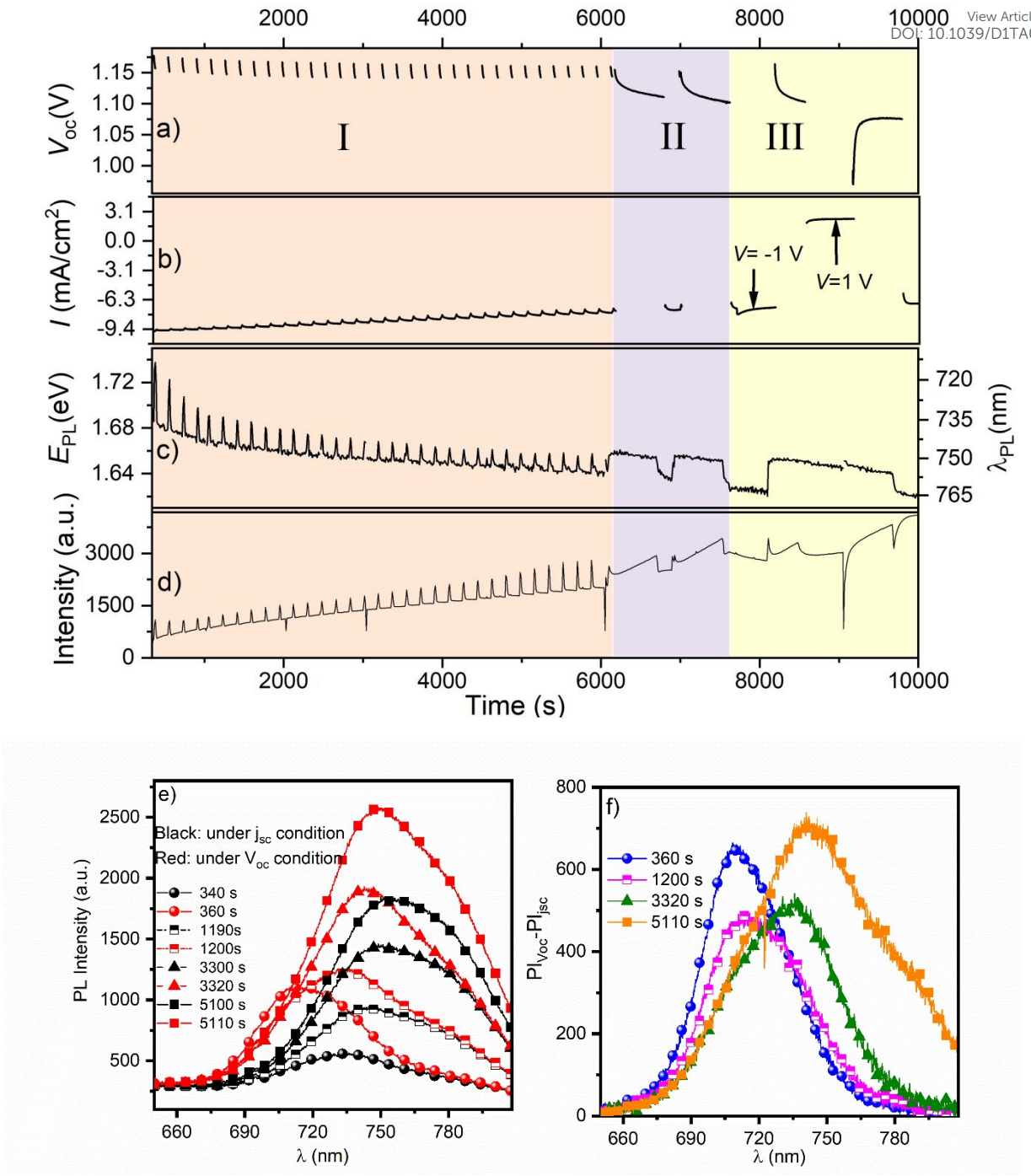

Figure 2. Light-soaking experiment of a device containing $Cs_{0.1}FA_{0.9}Pb(I_{0.65}Br_{0.35})_3$ for 10000 s. In region I, the device is mainly kept at short circuit and periodically (every 3 minutes) switched to open circuit. In region II, the device is kept at open circuit and switched to short circuit in between, and in region III the device is kept at the denoted voltages followed by some time under open circuit. (a) V_{oc}, (b) current density, (c) energy of the PL maximum, (d) counts at the PL maximum. (e) Samples of spectra during region I, under short circuit (black) and the subsequent open circuit condition (red). (f) Subtraction of the spectra under open and short circuit of panel e).

We perform a similar experiment on devices with the mixed halide composition and observe a much more complex behavior. We start with light-soaking under short circuit, as it appeared to have less influence on the V_{oc}. We monitor the short-circuit current density (J_{sc}) and PL continuously, and V_{oc} periodically every 3 minutes (**Fig. 2,** region I). We observe an increase in the PL intensity (Fig. 2d), both

View Article Online
DOI: 10.1039/D1TA02878B

under open and short circuit, whereas the V_{oc} remains almost unmodified (Fig. 2a). At the same time the PL red-shifts continuously (Fig. 2c), from around 720 to 770 nm, corresponding to a shift of the I:Br from 0.65:0.35 to 0.8:0.2[31,32]. This shift has been observed on films as well (Fig. SI2b) and represents the well-documented characteristics of phase segregation[8] facilitated by halide vacancy migration.[33–35] In particular iodine migration is reported to be enhanced by illumination.[36] The exact mechanisms are still under investigation, with reports ranging from thermodynamic considerations[37] to localized polarons that induce lattice strains,[38] to positive charge e.g. prevalent at grain boundaries,[12] to kinetic modeling considering a demixing threshold intensity,[39] to gradients in the absorption profile.[23]

Interestingly, we observe that the shifted PL does not affect the V_{oc} despite the lower bandgap phase forming that is assumed to act as a kind of "trap" or "defect".[8] One might suspect that the higher yield and the lower bandgap compensate each other and lead to a stable V_{oc}. However, this does not seem to quantitatively match the observations. (A rigorous quantification would require an accurate measurement of the absorption onset to exclude broader tails as done in some very recent study[40] and further elaborated on in the discussion part of this work.) Furthermore, one might suspect that V_{oc} is entirely limited by the contact materials and is therefore resistant against this low-energy phase. However, this is unlikely as the initial V_{oc} difference between single-halide device (0.95 V) and mixed halide device (1.14 V) equals the difference in bandgap/*e* (0.19 V).

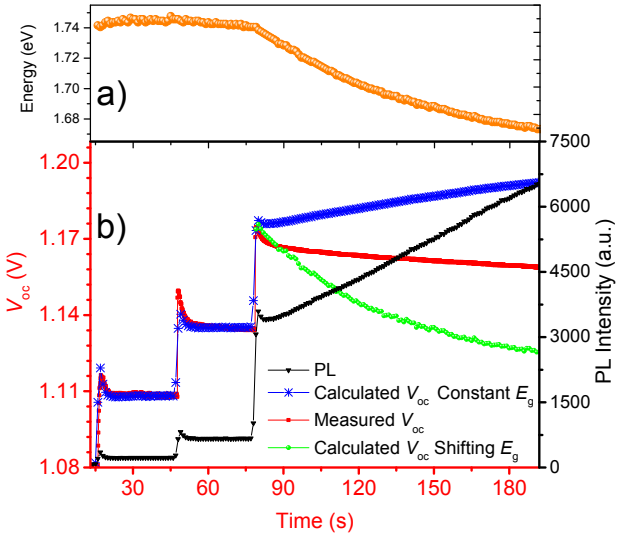

Figure 3. (a) Peak energy shift during light soaking. (b) Evolution of open-circuit voltage (V_{oc}) and PL intensity during light-soaking of a mixed-halide device under three light intensities (2.5, 5, 12.5 mW/mm^2) changed at 45 and 75 s. Independent of halide segregation (visible only for the highest light intensity), the V_{oc} (red) shows a comparable transient upon the light intensity is changed, which can only be reproduced by the PL (blue) as long as phase segregation does not happen. The green curve depicts a calculated V_{oc} assuming that the shift in peak energy (a) would cause the same shift in band gap and affect V_{oc}.

Further experiments show that the trend in V_{oc} is not directly correlated to the changes in PL which are related to phase segregation. E.g. keeping the device at V_{oc} (Fig. 2 region II), leads to a reversible strong decrease of V_{oc} (Fig. 2a), as is the case for non-halide-phase separation devices, whereas the PL just continues the rise and red-shift (Fig. 2c,d). Also applying bias voltages in reverse or forward does not considerably affect the trend of PL shift and cannot invert it (region III). However, the kinetics are

View Article Online
DOI: 10.1039/D1TA02878B

slightly enhanced, as seen in a faster shift (Fig. 2c) and increase of PL (Fig. 2d) under open circuit, which could be due to charge-carrier enhanced phase separation.[41–43] The discrepancy of PL and V_{oc} becomes obvious under light-soaking at open circuit, where V_{oc} decreases by around 50 mV, whereas the PL shifts by only 10 meV and the intensity even increases. Region III in Fig. 2 ultimately shows that changes in V_{oc} are not correlated to changes in PL, as the PL shifts monotonically even in the case of increasing V_{oc}. Therefore, a causal relation between V_{oc} and shifted PL due to phase segregation as reported in ref. [17] would require more evidence. We further confirmed that the formation of the low-gap phase is not the reason for a decreased V_{oc} by monitoring PL and V_{oc} at different illumination intensity. In such an experiment we can probe the V_{oc} response of our mixed halide device without inducing halide phase segregation (exploiting the known dependence of phase segregation on light intensity including a threshold intensity[39]). Figure 3 shows that the V_{oc} upon change of light intensity follows similar transients, independent of whether phase segregation sets in or not. Whereas the V_{oc} roughly follows what is expected from PL prior to phase segregation (similar to Fig. 1), the trend in V_{oc} remains even when phase segregation sets in and calculated and measured V_{oc} diverge, resulting in an underestimation of V_{oc}, when assuming that the low-gap phase limits V_{oc} (green line). Therefore, we can conclude from the very same sample that the trends seen in V_{oc} are not correlated with the occurrence of light-induced halide segregation.

Is this trend in V_{oc}, which is not predictable from the PL, in contradiction to what has been outlined in the introduction? No, it is not. The reason is that the measured PL signal hardly depends on the applied voltage and the observed increase of the PL intensity happens not only at V_{oc} but also at J_{sc}. Therefore, it might be advisable to investigate the difference between the PL under V_{oc} and the previous J_{sc}. This data can be deduced from the spikes in Fig. 2d and seems to change marginally. Besides the spikes in intensity, the evolution of the spectrum shows an interesting feature: Additionally to the continuous overall red-shift, it always remains blue-shifted when measured under open circuit compared to short circuit ("spikes" and steps in Fig. 2c). **Fig. 2e** shows spectra selected during light-soaking under short circuit (region I). Subtracting subsequent spectra at short circuit from those at open circuit, the remaining intensity stays rather unmodified and the red-shift is less-pronounced (inset). Therefore, the emerging low-energy PL due to phase segregation is rather independent of the operating voltage, i.e. it is hardly quenched at J_{sc}. This is different to an effect reported in ref. [7], where a large gradient in quasi-Fermi levels leads to discrepancies between the chemical potential deduced from PL and V_{oc}.

View Article Online
DOI: 10.1039/D1TA02878B

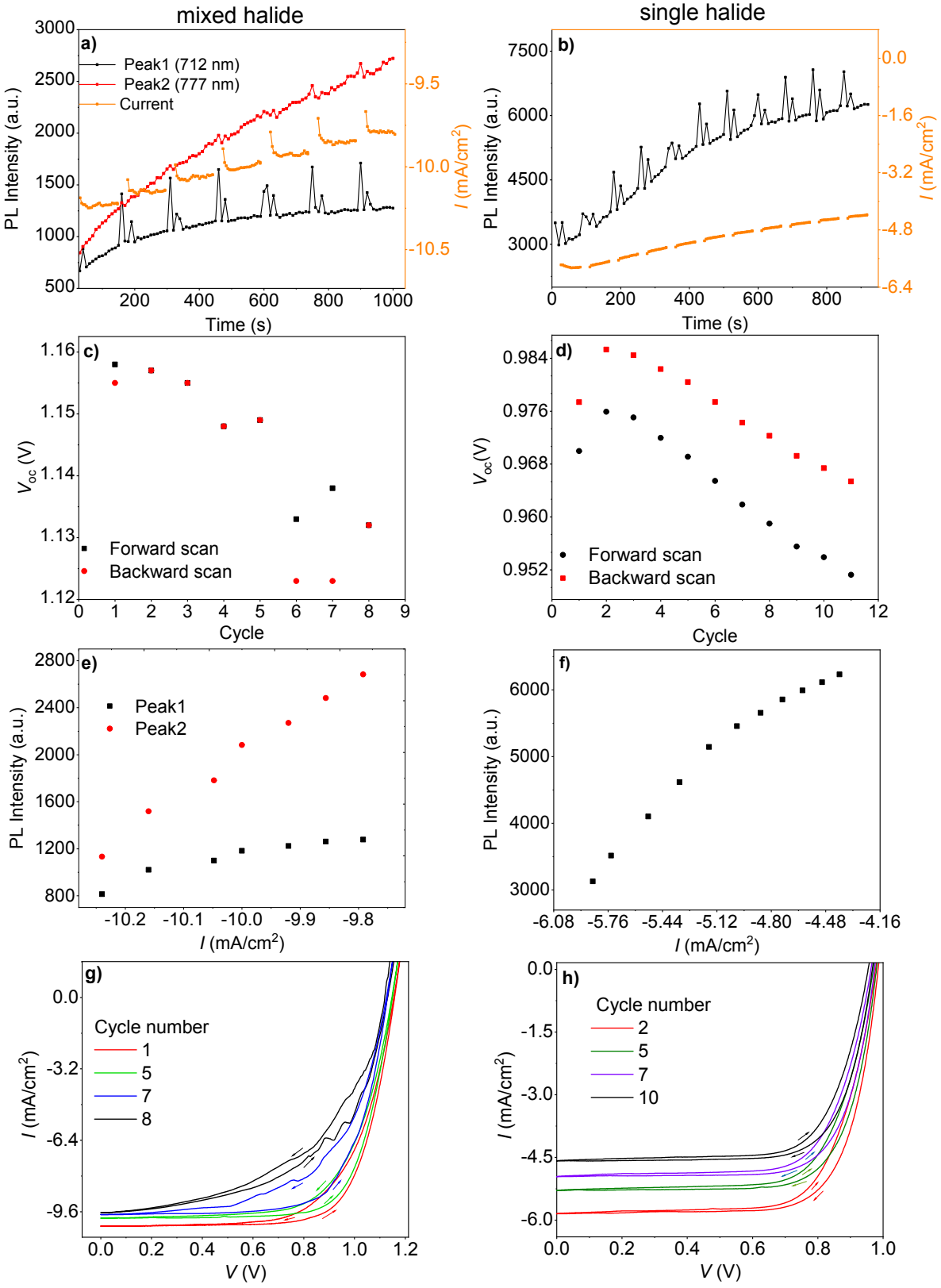

Figure 4. Light-soaking under short circuit with periodical interruptions for *JV* scans (from 0 V to 1.2 V and back, every ≈ 2 minutes) for devices with mixed halide (left) and single halide (right) perovskite. (a,b) PL signal at the selected wavelengths and the photocurrent. (c,d) Open-circuit voltage extracted

View Article Online
DOI: 10.1039/D1TA02878B

from the *JV* curves (e,f) PL intensity vs. current, (g,h) *JV* curves recorded with a sweep rate of 100 mV/s starting from forward bias.

The difference in PL signals under open circuit and short circuit are important for the following discussions. It is also visible in another measurement series, where light-soaking at short circuit was periodically interrupted by *JV* scans. The PL counts are plotted for two selected wavelengths (**Fig. 4a**), showing the expected stronger increase at 777 nm due to the red-shift during light-soaking, while V_{oc} decreases (Fig. 4c). During the *JV* scan, the emission at this wavelength is not affected in contrast to the one at 712 nm, which shows an increase when the device is at/closer to open circuit. Based on these observations, we conclude that the low-gap phase, which is more emissive, hardly contributes to the photovoltaic response of the device. We hypothesize that it forms nanoscopic regions that are rather insulated from the photovoltaically active part. In this case, the common one-dimensional models are not sufficient to describe device operation. This idea is consistent with a voltage-independent loss in photocurrent during light soaking that correlates roughly linearly with the increased PL of the low energy phase (peak 2 at 777 nm) (Fig. 4e).

As **Fig. 4b** and d show, this decrease in current and voltage is not unique to devices with mixed halides. It can occur at instable single-halide devices as well, which show a decrease of J_{sc} concomitant with an enhancement of PL (Fig. 3b,f). This behavior can be explained with ion migration, where smallest changes during film fabrication can result e.g. in varied concentrations of halide defects. As there is no peak shift, we can straightforwardly conclude that the PL intensity does not correlate with V_{oc}. Therefore, also in single-halide systems, these inactive regions can form. As not only V_{oc} decreases but at the same time the PL increases, this effect cannot be solely attributed to an enhanced recombination at the contacts, which could explain a divergence of PL yield and V_{oc}.[7] Interestingly, the photocurrent of these regions can be recovered when performing a fast reverse scan after a positive pre-bias, indicating that these regions can contribute to current, when the electric field is sufficient to extract these charges.[44] We can conclude that the decrease in current (independent of halide phase-segregation) is not caused by an enhanced (non-radiative) recombination but by the formation of isolated luminescent regions. The only qualitative difference in the current-voltage characteristics between devices with and without halide-segregation is the hysteresis. Devices with halide segregation often show inverted hysteresis (Fig. 4g,h), commonly attributed to ion migration and energy barriers close to the contacts.[45,46]

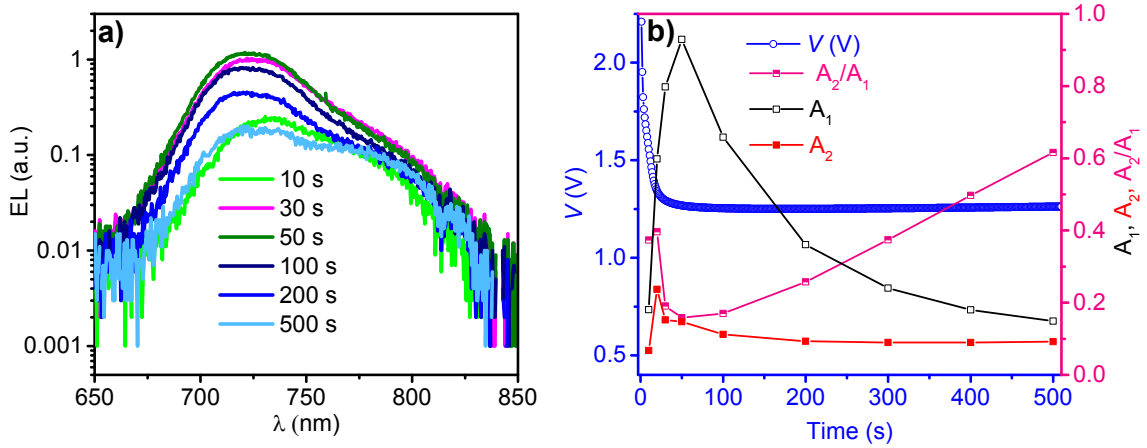

Figure 5. Continuous EL measurement of $Cs_{0.1}FA_{0.9}Pb(I_{0.65}Br_{0.35})_3$ device during applying a constant current of 2 mA (≈ 7 mA/cm²). (a) Evolution of EL spectra (b) Driving voltage and development of

View Article Online
DOI: 10.1039/D1TA02878B

amplitudes and their ratio of high energy peak (1: 725 nm) low energy peak (2: 776 nm) obtained by fitting two Gaussians.

The above applied optical reciprocity between photoluminescence and electrochemical potentials in the absorber allows for a direct comparison with V_{oc} only in the case of flat quasi-Fermi levels, as already mentioned. However, Rau's more general optoelectronic reciprocity relation[47] provides a direct description of V_{oc} as a function of EL spectra and yield. Therefore, in the following we investigate the evolution of electroluminescence spectra. First we perform continuous EL measurements under an applied current density of 7 mA/cm^2 and monitor the applied voltage. Commonly and for our reference device (Fig. SI7a), the EL spectrum in these perovskite devices is widely identical to the PL as expected for a classical semiconductor with a well-defined bandgap.[4,48] During the measurement, the EL intensity decreases, which is a well-known unresolved degradation phenomenon for perovskite solar cells and LEDs.[49] However, the spectral shape does not change (Fig. SI7b). This is in contrast to devices with halide phase segregation, which additionally show changes in the EL spectra (Fig. 5a). It appears as the emission can be described by an overlap of two contributions, one with a maximum at 776 nm (where the PL usually stabilizes after long light-soaking) and the other one at around 725 nm. How pronounced the low-energy contribution is, depends on whether the sample has already seen some light or whether the initial film was not perfectly mixed. Interestingly, during applying current, the high-energy peak decreases strongly, whereas the low-energy peak remains rather unmodified. We can quantify this trend by fitting two Gaussians. The results (Fig. 5b) show that the changes in the EL spectrum can be explained by changes of the relative contributions of the two peaks with unmodified maxima and width (Table SI2). Except for an initial increase of the EL and decrease of the driving voltage (possibly due to a more balanced charge injection upon ion migration[27,50]), the EL decreases as for any perovskite device. As we do not observe a red-shift, we can conclude that application of such a current and voltage does not lead to halide phase segregation. This observation does not reproduce reports on current-induced changes of EL[51] and PL[43] spectra. The reason might be harsher conditions applied in the literature rationalized by a possible acceleration of phase-segregation by higher applied voltages.[52]

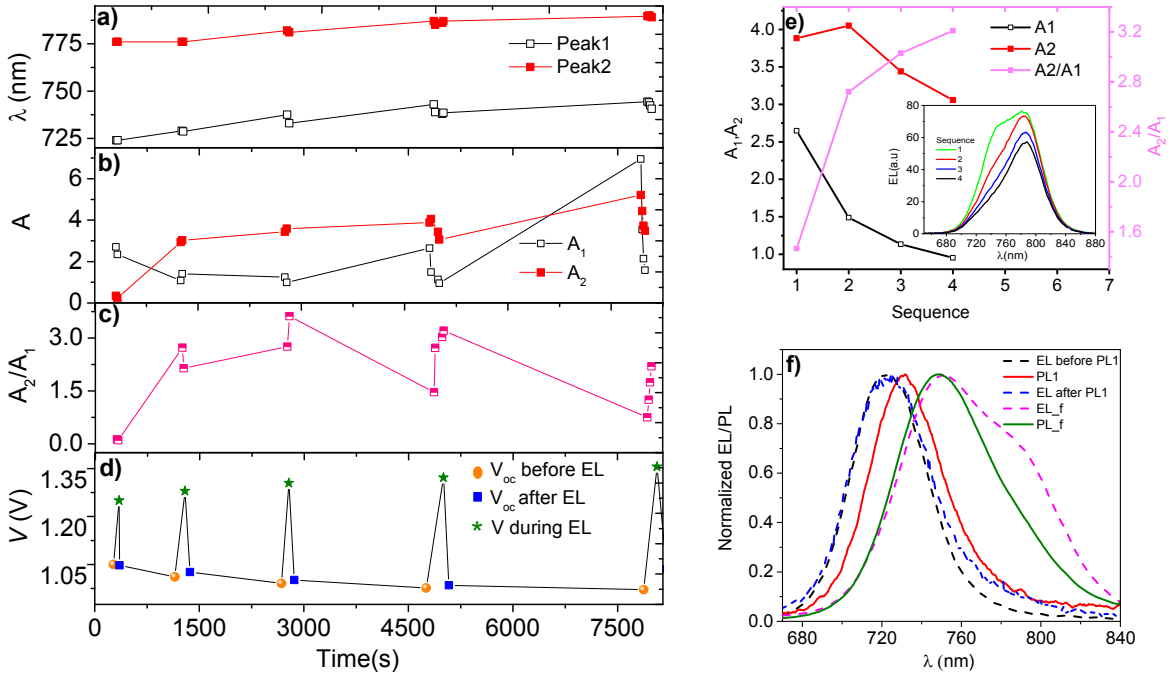

View Article Online
DOI: 10.1039/D1TA02878B

Figure 6. Evolution of EL during light-soaking of $Cs_{0.1}FA_{0.9}Pb(I_{0.65}Br_{0.35})_3$ device, which is interrupted at 310 s, 1250 s, 2760 s, 4860 s and 7930 s to measure EL spectra. (a) Wavelength of the maxima obtained by a fit with two Gaussians of amplitude A_1 and A_2 (b). (c) Development of the open circuit voltage during light soaking and the voltage needed to drive the constant current for EL. Lines connect the measurement dots to visualize the sequence. (d) Example for subsequent EL measurements (every 20 s) at time 4860 s. (e) Comparison of EL and PL at the beginning (labeled "1") of the experiment and at the end (labeled "f").

In a final measurement we want to investigate how EL spectra change during light soaking and compare them to PL and the V_{oc}. Herby we interrupt the light soaking experiment and apply a current (7 mA/cm^2) to measure a few (2 to 4) EL spectra. During such a set of EL measurements, the same trend is observed as in Fig. 5 (stable or slightly backward shifting peak positions but changed ratios of the two peaks, Fig. 6e). During light soaking, however and in contrast to the data in ref.[53], the EL spectra shift (Fig. 6a, given a homogeneous illumination of the active area) following the above discussed trend of the PL shift. However, in contrast to PL, EL intensity does not considerably increase (Fig. 6b) and a more stabilized value obtained after two or three EL measurements ($\approx$ 1 min.) remains rather constant. The voltage required to drive the current is plotted in Fig. 6d (green stars). Its increase indicates an enhanced resistance, which most likely results from phase-segregated domains. In contrast, commonly a decreased EL and V_{oc} come along with a decreased driving voltage due to enhanced recombination in the device.

The expected decrease of V_{oc} during the light soaking experiment is documented in Fig. 6d as well. The complex shape of the EL, including a shift of the two peaks and only slight changes in the relative intensity during light-soaking, and a strongly variable EL intensity of subsequent EL measurements in a series, does not allow us to make a strong statement whether the reciprocity relation between V_{oc} and EL is applicable. However, comparing the V_{oc} before and after the EL series, we can conclude that similar to PL, the EL information does not describe the trend in the V_{oc}: V_{oc} is always higher after the EL measurement (blue square) than before (orange circle). However, the EL intensity decreases during the EL measurement. The peaks do not shift but the relative contribution of the low energy peak becomes more prominent. Therefore, we would expect a decrease of V_{oc} (overall lower yield, emission predominantly at lower energy), which we do not observe.

To complete the data, we compare EL and PL spectra at the same stage of light soaking and confirm the trend we expect from the maxima position of Fig. 6a. However, PL and EL spectra are not identical. The PL tends to be more red-shifted, already at the beginning of the experiment (red curve). An attempt of fitting the spectra after light soaking with two peaks, yields an excellent fit for EL (as for data of Fig. 5) but not for the PL, where the low-energy regime is much broader. The positions of the high-energy peak between PL and EL match. Note that EL and PL spectra do not depend on light intensity and driving current, respectively (Fig. SI8), making the difference between PL and EL spectra an intrinsic difference between the two experiments.

Discussion

We want to discuss our key findings related to device performance and compare them to most recent studies, without overinterpreting speculative microscopic origins related to our findings, which cannot be unraveled with our measurements.

Comparing PL spectra under short circuit and open circuit we identified that the emerging low-gap-phase PL is less quenched at short circuit, indicating that these charges contribute less to photocurrent. Our findings are therefore consistent with small I rich domains in the bulk as observed in ref. [54], where the authors found that phase segregation is an intrinsic material property that is not predominantly

View Article Online
DOI: 10.1039/D1TA02878B

influenced by the microstructure. Such iodine rich clusters are also predicted from microscopic calculations.[55]

Whereas the PL signal cannot easily be used to quantify the amount of phase segregation due to unknown changes in the PL yields and charge carrier diffusion, X-ray diffraction (XRD)[32,56] and absorption measurements[8] have been used to quantify the low-gap iodine-rich phase. On the other hand, FTPS measurements,[12] where the photocurrent is measured spectrally resolved, might not be the optimum choice to quantify the amount of low-gap phase if our hypothesis is correct that the low-gap phase contributes less to photocurrent. Furthermore, our observation of EL and PL spectra that are different and evolve differently, together with the involvement of inhomogeneities in the absorber complicates a V_{oc} analysis based on a detailed-balance approach based on Rau's reciprocity[47] of photovoltaic quantum efficiency from FTPS and electroluminescence data as presented in ref. [40]. The difference in EL and PL indicates that charges are not (completely) equilibrated between the phases and the energy-funneling[57] during PL experiments is not complete. The non-applicability of the reciprocity relation between the EL and V_{oc} also supports the generation of photovoltaically inactive regions. This interpretation is consistent with theoretical work based on 1D drift-diffusion simulations, where Kirchartz et al[58] show that for a low mobility, predicted and measured (there simulated) V_{oc} do not coincide. We note that our case cannot be described by a low mobility in the overall absorber as this would lead to a strong voltage dependence of the charge carrier collection efficiency and thus a low FF, which we do not observe. However, we regard the interfaces between the major phase and our nanoscopic regions as source of a low mobility for charges on the nanoscopic regions.

Coming back to the PL, we could not identify that the onset and transients of halide segregation caused changes in V_{oc} during light-soaking. Instead, a major source of instability is not the high Br content itself but a more general instability, e.g. due to varied crystallinity[59] or ion migration,[60] which occurs in our reference device as well.

For devices with higher Br content, a major culprit for a high V_{oc} loss is non-radiative recombination. This is confirmed by investigating $MAPbBr_3$, where halide migration does not occur and the PL and EL maxima at 535 nm are close to the absorption onset (Fig. SI9-10). The V_{oc} is around 1.5 V corresponding to a voltage deficit of ca. 0.8 V and coming along with a low EL external quantum yield (EQE_{EL}) in the order of 10^{-8} (Table SI3). Measuring the EQE_{EL} for mixed halide compositions with high Br content (Br:I = 1:1 and 2:1), we observe similarly low values, which confirms an additional voltage loss of ca. 300 mV compared to iodine-rich compositions with EQE_{EL} in the order of 0.1 to 1%. This loss is attributed to enhanced non-radiative recombination,[61,62] which occurs independent of phase segregation and photo-induced changes in the PL intensity (Fig. SI11). It is to some extent present in the film as well,[63] where we observe less stable PL for the $MAPbBr_3$ (Fig. SI12) compared to iodine compositions (Fig. SI2a). Therefore, the challenge is not only about stopping phase segregation but to identify and possibly eliminate defects in Br-rich compositions and in a final step avoid recombination at interfaces with the charge-transport layers. This finding is consistent with very recent studies, attributing the major loss of mixed-halide compositions with higher Br content to enhanced non radiative recombination.[40,53]

Conclusion

In conclusion, we have investigated the correlation of changes in the photo- and electroluminescence and solar cell parameters in perovskite solar cells with and without halide phase segregation. We have found that there is no causal correlation between the observed changes in the open-circuit voltage and the formation of emissive iodide-rich low-energy states. These regions seem to not dominate recombination of charge carriers at open circuit but at short circuit, where photoluminescence from

the low-gap phase is less quenched. We have hypothesized that this is due to the fact that the iodide-rich regions become partially insulated from the rest of the material. This also explains why the reciprocity relation of electroluminescence and open-circuit voltage was not readily applicable. A similar effect of generation of high-luminescence regions upon light soaking can occur in single-halide perovskites as well, indicating that the low open-circuit voltage of mixed compositions and changes upon light-soaking are related to non-radiative recombination in the device and predominantly at the contacts. A comparison with $MAPbBr_3$ confirms that Br(-rich) perovskite solar cells in general suffer from higher non-radiative recombination losses. Our results show that for an accurate description of our devices, a one-dimensional device simulation would not be sufficient, a conclusion which becomes particularly relevant when (reversible and irreversible) aging effects are to be explained quantitatively, which are one of the most challenging remaining questions in the perovskite photovoltaics community.

References

1. Shockley, W. & Queisser, H. J. Detailed Balance Limit of Efficiency of p-n Junction Solar Cells. *J. Appl. Phys.* **32,** 510–519 (1961).
2. Ross, R. T. Some Thermodynamics of Photochemical Systems. *J. Chem. Phys.* **46,** 4590–4593 (1967).
3. Tress, W. Perovskite Solar Cells on the Way to Their Radiative Efficiency Limit – Insights Into a Success Story of High Open-Circuit Voltage and Low Recombination. *Adv. Energy Mater.* **7,** 1602358 (2017).
4. Tress, W., Marinova, N., Inganäs, O., Nazeeruddin, Mohammad. K., Zakeeruddin, S. M. & Graetzel, M. Predicting the Open-Circuit Voltage of CH3NH3PbI3 Perovskite Solar Cells Using Electroluminescence and Photovoltaic Quantum Efficiency Spectra: the Role of Radiative and Non-Radiative Recombination. *Adv. Energy Mater.* **5,** 140812 (2015).
5. Liu, Z., Krückemeier, L., Krogmeier, B., Klingebiel, B., Márquez, J. A., Levcenko, S., Öz, S., Mathur, S., Rau, U., Unold, T. & Kirchartz, T. Open-Circuit Voltages Exceeding 1.26 V in Planar Methylammonium Lead Iodide Perovskite Solar Cells. *ACS Energy Lett.* **4,** 110–117 (2019).
6. Stolterfoht, M., Caprioglio, P., Wolff, C. M., Márquez, J. A., Nordmann, J., Zhang, S., Rothhardt, D., Hörmann, U., Redinger, A., Kegelmann, L., Albrecht, S., Kirchartz, T., Saliba, M., Unold, T. & Neher, D. The perovskite/transport layer interfaces dominate non-radiative recombination in efficient perovskite solar cells. *ArXiv181001333 Phys.* (2018). at <http://arxiv.org/abs/1810.01333>
7. Caprioglio, P., Stolterfoht, M., Wolff, C. M., Unold, T., Rech, B., Albrecht, S. & Neher, D. On the Relation between the Open-Circuit Voltage and Quasi-Fermi Level Splitting in Efficient Perovskite Solar Cells. *Adv. Energy Mater.* **9,** 1901631 (2019).
8. Hoke, E. T., Slotcavage, D. J., Dohner, E. R., Bowring, A. R., Karunadasa, H. I. & McGehee, M. D. Reversible photo-induced trap formation in mixed-halide hybrid perovskites for photovoltaics. *Chem. Sci.* **6,** 613–617 (2014).
9. Nandi, P., Giri, C., Swain, D., Manju, U., Mahanti, S. D. & Topwal, D. Temperature Dependent Photoinduced Reversible Phase Separation in Mixed-Halide Perovskite. *ACS Appl. Energy Mater.* **1,** 3807–3814 (2018).
10. Zhou, W., Zhao, Y., Zhou, X., Fu, R., Li, Q., Zhao, Y., Liu, K., Yu, D. & Zhao, Q. Light-Independent Ionic Transport in Inorganic Perovskite and Ultrastable Cs-Based Perovskite Solar Cells. *J. Phys. Chem. Lett.* **8,** 4122–4128 (2017).
11. Zhou, Y., Jia, Y.-H., Fang, H.-H., Loi, M. A., Xie, F.-Y., Gong, L., Qin, M.-C., Lu, X.-H., Wong, C.-P. & Zhao, N. Composition-Tuned Wide Bandgap Perovskites: From Grain Engineering to Stability and Performance Improvement. *Adv. Funct. Mater.* **28,** 1803130 (2018).
12. Tang, X., van den Berg, M., Gu, E., Horneber, A., Matt, G. J., Osvet, A., Meixner, A. J., Zhang, D. & Brabec, C. J. Local Observation of Phase Segregation in Mixed-Halide Perovskite. *Nano Lett.* **18,** 2172–2178 (2018).

13. Gualdrón-Reyes, Andrés. F., Yoon, S. J., Barea, E. M., Agouram, S., Muñoz-Sanjosé, V., Meléndez, Á. M., Niño-Gómez, M. E. & Mora-Seró, I. Controlling the Phase Segregation in Mixed Halide Perovskites through Nanocrystal Size. *ACS Energy Lett.* **4,** 54–62 (2019).
14. Anizelli, H. S., Fernandes, R. V., Scarmínio, J., da Silva, P. R. C., Duarte, J. L. & Laureto, E. Effect of pressure on the remixing process in CH3NH3Pb(I1-xBrx)3 perovskite thin films. *J. Lumin.* **199,** 348–351 (2018).
15. Huang, W., Yoon, S. J. & Sapkota, P. Effect of Light Illumination on Mixed Halide Lead Perovskites: Reversible or Irreversible Transformation. *ACS Appl. Energy Mater.* **1,** 2859–2865 (2018).
16. Samu, G. F., Janáky, C. & Kamat, P. V. A Victim of Halide Ion Segregation. How Light Soaking Affects Solar Cell Performance of Mixed Halide Lead Perovskites. *ACS Energy Lett.* **2,** 1860–1861 (2017).
17. Bush, K. A., Frohna, K., Prasanna, R., Beal, R. E., Leijtens, T., Swifter, S. A. & McGehee, M. D. Compositional Engineering for Efficient Wide Band Gap Perovskites with Improved Stability to Photoinduced Phase Segregation. *ACS Energy Lett.* **3,** 428–435 (2018).
18. Knight, A. J., Patel, J. B., Snaith, H. J., Johnston, M. B. & Herz, L. M. Trap States, Electric Fields, and Phase Segregation in Mixed-Halide Perovskite Photovoltaic Devices. *Adv. Energy Mater.* **10,** 1903488 (2020).
19. Belisle, R. A., Bush, K. A., Bertoluzzi, L., Gold-Parker, A., Toney, M. F. & McGehee, M. D. Impact of Surfaces on Photoinduced Halide Segregation in Mixed-Halide Perovskites. *ACS Energy Lett.* **3,** 2694–2700 (2018).
20. Saliba, M., Matsui, T., Seo, J.-Y., Domanski, K., Correa-Baena, J.-P., Nazeeruddin, M. K., Zakeeruddin, S. M., Tress, W., Abate, A., Hagfeldt, A. & Grätzel, M. Cesium-containing triple cation perovskite solar cells: improved stability, reproducibility and high efficiency. *Energy Environ. Sci.* **9,** 1989–1997 (2016).
21. Cappel, U. B., Svanström, S., Lanzilotto, V., Johansson, F. O. L., Aitola, K., Philippe, B., Giangrisostomi, E., Ovsyannikov, R., Leitner, T., Föhlisch, A., Svensson, S., Mårtensson, N., Boschloo, G., Lindblad, A. & Rensmo, H. Partially Reversible Photoinduced Chemical Changes in a Mixed-Ion Perovskite Material for Solar Cells. *ACS Appl. Mater. Interfaces* **9,** 34970–34978 (2017).
22. Svanström, S., Jacobsson, T. J., Sloboda, T., Giangrisostomi, E., Ovsyannikov, R., Rensmo, H. & Cappel, U. B. Effect of halide ratio and Cs+ addition on the photochemical stability of lead halide perovskites. *J. Mater. Chem. A* **6,** 22134–22144 (2018).
23. Barker, A. J., Sadhanala, A., Deschler, F., Gandini, M., Senanayak, S. P., Pearce, P. M., Mosconi, E., Pearson, A. J., Wu, Y., Srimath Kandada, A. R., Leijtens, T., De Angelis, F., Dutton, S. E., Petrozza, A. & Friend, R. H. Defect-Assisted Photoinduced Halide Segregation in Mixed-Halide Perovskite Thin Films. *ACS Energy Lett.* **2,** 1416–1424 (2017).
24. Andaji-Garmaroudi, Z., Abdi-Jalebi, M., Guo, D., Macpherson, S., Sadhanala, A., Tennyson, E. M., Ruggeri, E., Anaya, M., Galkowski, K., Shivanna, R., Lohmann, K., Frohna, K., Mackowski, S., Savenije, T. J., Friend, R. H. & Stranks, S. D. A Highly Emissive Surface Layer in Mixed-Halide Multication Perovskites. *Adv. Mater.* **0,** 1902374
25. Hu, Y., Aygüler, M. F., Petrus, M. L., Bein, T. & Docampo, P. Impact of Rubidium and Cesium Cations on the Moisture Stability of Multiple-Cation Mixed-Halide Perovskites. *ACS Energy Lett.* **2,** 2212–2218 (2017).
26. Domanski, K., Alharbi, E. A., Hagfeldt, A., Grätzel, M. & Tress, W. Systematic investigation of the impact of operation conditions on the degradation behaviour of perovskite solar cells. *Nat. Energy* **3,** 61–67 (2018).
27. Tress, W., Yavari, M., Domanski, K., Yadav, P., Niesen, B., Baena, J. P. C., Hagfeldt, A. & Graetzel, M. Interpretation and evolution of open-circuit voltage, recombination, ideality factor and subgap defect states during reversible light-soaking and irreversible degradation of perovskite solar cells. *Energy Environ. Sci.* **11,** 151–165 (2018).
28. Tress, W. *Organic Solar Cells*. **208,** (Springer International Publishing, 2014).

29. Tress, W., Leo, K. & Riede, M. Influence of Hole-Transport Layers and Donor Materials on Open-Circuit Voltage and Shape of I–V Curves of Organic Solar Cells. *Adv. Funct. Mater.* **21,** 2140–2149 (2011).
30. Schelhas, L. T., Li, Z., Christians, J. A., Goyal, A., Kairys, P., Harvey, S. P., Kim, D. H., Stone, K. H., Luther, J. M., Zhu, K., Stevanovic, V. & Berry, J. J. Insights into operational stability and processing of halide perovskite active layers. *Energy Environ. Sci.* **12,** 1341–1348 (2019).
31. Eperon, G. E., Stranks, S. D., Menelaou, C., Johnston, M. B., Herz, L. M. & Snaith, H. J. Formamidinium lead trihalide: a broadly tunable perovskite for efficient planar heterojunction solar cells. *Energy Environ. Sci.* **7,** 982–988 (2014).
32. Brennan, M. C., Draguta, S., Kamat, P. V. & Kuno, M. Light-Induced Anion Phase Segregation in Mixed Halide Perovskites. *ACS Energy Lett.* **3,** 204–213 (2018).
33. Yang, T.-Y., Gregori, G., Pellet, N., Grätzel, M. & Maier, J. The Significance of Ion Conduction in a Hybrid Organic–Inorganic Lead-Iodide-Based Perovskite Photosensitizer. *Angew. Chem.* **127,** 8016–8021 (2015).
34. Ruth, A., Brennan, M. C., Draguta, S., Morozov, Y. V., Zhukovskyi, M., Janko, B., Zapol, P. & Kuno, M. Vacancy-Mediated Anion Photosegregation Kinetics in Mixed Halide Hybrid Perovskites: Coupled Kinetic Monte Carlo and Optical Measurements. *ACS Energy Lett.* **3,** 2321–2328 (2018).
35. Yoon, S. J., Kuno, M. & Kamat, P. V. Shift Happens. How Halide Ion Defects Influence Photoinduced Segregation in Mixed Halide Perovskites. *ACS Energy Lett.* **2,** 1507–1514 (2017).
36. Kim, G. Y., Senocrate, A., Yang, T.-Y., Gregori, G., Grätzel, M. & Maier, J. Large tunable photoeffect on ion conduction in halide perovskites and implications for photodecomposition. *Nat. Mater.* **17,** 445–449 (2018).
37. Brivio, F., Caetano, C. & Walsh, A. Thermodynamic Origin of Photoinstability in the CH3NH3Pb(I1–xBrx)3 Hybrid Halide Perovskite Alloy. *J. Phys. Chem. Lett.* **7,** 1083–1087 (2016).
38. Bischak, C. G., Hetherington, C. L., Wu, H., Aloni, S., Ogletree, D. F., Limmer, D. T. & Ginsberg, N. S. Origin of Reversible Photoinduced Phase Separation in Hybrid Perovskites. *Nano Lett.* **17,** 1028–1033 (2017).
39. Draguta, S., Sharia, O., Yoon, S. J., Brennan, M. C., Morozov, Y. V., Manser, J. S., Kamat, P. V., Schneider, W. F. & Kuno, M. Rationalizing the light-induced phase separation of mixed halide organic–inorganic perovskites. *Nat. Commun.* **8,** 200 (2017).
40. Mahesh, S., Ball, J. M., Oliver, R. D. J., McMeekin, D. P., Nayak, P. K., Johnston, M. B. & Snaith, H. J. Revealing the origin of voltage loss in mixed-halide perovskite solar cells. *Energy Environ. Sci.* **13,** 258–267 (2020).
41. Lin, Y., Chen, B., Fang, Y., Zhao, J., Bao, C., Yu, Z., Deng, Y., Rudd, P. N., Yan, Y., Yuan, Y. & Huang, J. Excess charge-carrier induced instability of hybrid perovskites. *Nat. Commun.* **9,** 4981 (2018).
42. Samu, G. F., Balog, Á., De Angelis, F., Meggiolaro, D., Kamat, P. V. & Janáky, C. Electrochemical Hole Injection Selectively Expels Iodide from Mixed Halide Perovskite Films. *J. Am. Chem. Soc.* **141,** 10812–10820 (2019).
43. Duong, T., Mulmudi, H. K., Wu, Y., Fu, X., Shen, H., Peng, J., Wu, N., Nguyen, H. T., Macdonald, D., Lockrey, M., White, T. P., Weber, K. & Catchpole, K. Light and Electrically Induced Phase Segregation and Its Impact on the Stability of Quadruple Cation High Bandgap Perovskite Solar Cells. *ACS Appl. Mater. Interfaces* **9,** 26859–26866 (2017).
44. Tress, W., Marinova, N., Moehl, T., Zakeeruddin, S. M., Nazeeruddin, M. K. & Grätzel, M. Understanding the rate-dependent J–V hysteresis, slow time component, and aging in CH3NH3PbI3 perovskite solar cells: the role of a compensated electric field. *Energy Environ. Sci.* **8,** 995–1004 (2015).
45. Tress, W., Correa Baena, J. P., Saliba, M., Abate, A. & Graetzel, M. Inverted Current–Voltage Hysteresis in Mixed Perovskite Solar Cells: Polarization, Energy Barriers, and Defect Recombination. *Adv. Energy Mater.* **6,** 1600396 (2016).

46. Shen, H., Jacobs, D. A., Wu, Y., Duong, T., Peng, J., Wen, X., Fu, X., Karuturi, S. K., White, T. P., Weber, K. & Catchpole, K. R. Inverted Hysteresis in CH3NH3PbI3 Solar Cells: Role of Stoichiometry and Band Alignment. *J. Phys. Chem. Lett.* **8,** 2672–2680 (2017).
47. Rau, U. Reciprocity relation between photovoltaic quantum efficiency and electroluminescent emission of solar cells. *Phys. Rev. B* **76,** 085303 (2007).
48. Tvingstedt, K., Malinkiewicz, O., Baumann, A., Deibel, C., Snaith, H. J., Dyakonov, V. & Bolink, H. J. Radiative efficiency of lead iodide based perovskite solar cells. *Sci. Rep.* **4,** 6071 (2014).
49. Tavakoli, M. M., Tress, W., Milić, J. V., Kubicki, D., Emsley, L. & Grätzel, M. Addition of adamantylammonium iodide to hole transport layers enables highly efficient and electroluminescent perovskite solar cells. *Energy Environ. Sci.* **11,** 3310–3320 (2018).
50. Ebadi, F., Taghavinia, N., Mohammadpour, R., Hagfeldt, A. & Tress, W. Origin of apparent light-enhanced and negative capacitance in perovskite solar cells. *Nat. Commun.* **10,** 1574 (2019).
51. Braly, I. L., Stoddard, R. J., Rajagopal, A., Uhl, A. R., Katahara, J. K., Jen, A. K.-Y. & Hillhouse, H. W. Current-Induced Phase Segregation in Mixed Halide Hybrid Perovskites and its Impact on Two-Terminal Tandem Solar Cell Design. *ACS Energy Lett.* **2,** 1841–1847 (2017).
52. Vashishtha, P. & Halpert, J. E. Field-Driven Ion Migration and Color Instability in Red-Emitting Mixed Halide Perovskite Nanocrystal Light-Emitting Diodes. *Chem. Mater.* **29,** 5965–5973 (2017).
53. Peña-Camargo, F., Caprioglio, P., Zu, F., Gutierrez-Partida, E., Wolff, C. M., Brinkmann, K., Albrecht, S., Riedl, T., Koch, N., Neher, D. & Stolterfoht, M. Halide Segregation versus Interfacial Recombination in Bromide-Rich Wide-Gap Perovskite Solar Cells. *ACS Energy Lett.* **5,** 2728–2736 (2020).
54. Bischak, C. G., Wong, A. B., Lin, E., Limmer, D. T., Yang, P. & Ginsberg, N. S. Tunable Polaron Distortions Control the Extent of Halide Demixing in Lead Halide Perovskites. *J. Phys. Chem. Lett.* **9,** 3998–4005 (2018).
55. Li, W., Rothmann, M. U., Liu, A., Wang, Z., Zhang, Y., Pascoe, A. R., Lu, J., Jiang, L., Chen, Y., Huang, F., Peng, Y., Bao, Q., Etheridge, J., Bach, U. & Cheng, Y.-B. Phase Segregation Enhanced Ion Movement in Efficient Inorganic CsPbIBr2 Solar Cells. *Adv. Energy Mater.* **7,** 1700946 (2017).
56. Sutter-Fella, C. M., Ngo, Q. P., Cefarin, N., Gardner, K. L., Tamura, N., Stan, C. V., Drisdell, W. S., Javey, A., Toma, F. M. & Sharp, I. D. Cation-Dependent Light-Induced Halide Demixing in Hybrid Organic–Inorganic Perovskites. *Nano Lett.* **18,** 3473–3480 (2018).
57. Yoon, S. J., Draguta, S., Manser, J. S., Sharia, O., Schneider, W. F., Kuno, M. & Kamat, P. V. Tracking Iodide and Bromide Ion Segregation in Mixed Halide Lead Perovskites during Photoirradiation. *ACS Energy Lett.* **1,** 290–296 (2016).
58. Kirchartz, T., Nelson, J. & Rau, U. Reciprocity between Charge Injection and Extraction and Its Influence on the Interpretation of Electroluminescence Spectra in Organic Solar Cells. *Phys. Rev. Appl.* **5,** 054003 (2016).
59. Rehman, W., McMeekin, D. P., Patel, J. B., Milot, R. L., Johnston, M. B., Snaith, H. J. & Herz, L. M. Photovoltaic mixed-cation lead mixed-halide perovskites: links between crystallinity, photo-stability and electronic properties. *Energy Environ. Sci.* **10,** 361–369 (2017).
60. Domanski, K., Roose, B., Matsui, T., Saliba, M., Turren-Cruz, S.-H., Correa-Baena, J.-P., Carmona, C. R., Richardson, G., Foster, J. M., Angelis, F. D., Ball, J. M., Petrozza, A., Mine, N., Nazeeruddin, M. K., Tress, W., Grätzel, M., Steiner, U., Hagfeldt, A. & Abate, A. Migration of cations induces reversible performance losses over day/night cycling in perovskite solar cells. *Energy Environ. Sci.* **10,** 604–613 (2017).
61. Zohar, A., Kulbak, M., Levine, I., Hodes, G., Kahn, A. & Cahen, D. What Limits the Open-Circuit Voltage of Bromide Perovskite-Based Solar Cells? *ACS Energy Lett.* 1–7 (2018). doi:10.1021/acsenergylett.8b01920
62. Arora, N., Dar, M. I., Hezam, M., Tress, W., Jacopin, G., Moehl, T., Gao, P., Aldwayyan, A. S., Deveaud, B., Grätzel, M. & Nazeeruddin, M. K. Photovoltaic and Amplified Spontaneous Emission Studies of High-Quality Formamidinium Lead Bromide Perovskite Films. *Adv. Funct. Mater.* **26,** 2846–2854 (2016).

63. Sutter-Fella, C. M., Li, Y., Amani, M., Ager, J. W., Toma, F. M., Yablonovitch, E., Sharp, I. D. & Javey, A. High Photoluminescence Quantum Yield in Band Gap Tunable Bromide Containing Mixed Halide Perovskites. *Nano Lett.* **16,** 800–806 (2016).

Author contributions

F.E. and B.Y. contributed equally. F.E. performed all the measurements and made the figures. B.Y. together with Y.K. prepared devices and films. W.T. analyzed and discussed the data together with F.E. and wrote the paper. A.H. supervised B.Y. and Y.K. N.T., R.M., and W.T. supervised F.E.

Acknowledgements

WT has received funding from the European Union's Horizon 2020 research and innovation programme under the ERC Starting Grant agreement no. 851676. Furthermore, funding by the Swiss National Science Foundation (Ambizione Energy grant no. PZENP2_173617) is kindly acknowledged. This project has furthermore received funding from the European Union's Horizon 2020 research and innovation programme under grant agreement No. 764047.

Experimental

Materials

Conductive glass, Fluorine-doped tin oxide (10 Ω/sq) is purchased from Nippon Sheet Glass, Titanium dioxide paste (30 NRD) is purchased from Dyesol. Dimethylformamide (DMF), dimethyl sulfoxide (DMSO) and chlorobenzene (CB) are purchased from Acros. Lead iodide is purchased from Alfa Aesar. Cesium iodide is purchased from TCI co, ltd. Formamidinium iodide and formamidinium bromide are purchased from Dyesol. N^2,N^2,$N^{2'}$,$N^{2'}$,N^7,N^7,$N^{7'}$,$N^{7'}$-octakis(4-methoxyphenyl)-9,9'-spirobi[9*H*-fluorene]-2,2',7,7'-tetramine (spiro-MeOTAD) is purchased from Dyesol. 4-*tert*-butyl pyridine, lithium bistrifluorosulfonyl imide (Li-TFSI), acetyl acetone, titanium diisopropoxide bis(acetylacetonate), 75 wt. % in isopropanol are purchased from Sigma-Aldrich. All the chemicals are used as received without further purification.

Device Fabrication

Substrate

Fluorine doped tin oxide (FTO) substrates (NSG-10) were chemically etched by zinc powder and 4 M HCl solution and sonicated in 2% Hellmanex water solution for 30 min, acetone for 15 min and ethanol for 15 min, respectively. Then, all substrates were further cleaned by UV-Ozone for 15 min.

Then, a compact TiO_2 layer was deposited on cleaned FTO substrates via spray pyrolysis deposition from a precursor solution of titanium diisopropoxide bis(acetylacetonate) in anhydrous ethanol, with oxygen as carrier gas. Substrates were heated at 450 ℃ and kept at this temperature for 15 min before and 30 min after the spray of the precursor solution, then left to cool down to room temperature. Mesoporous TiO_2 layer was spin-coated at 4000 rpm for 20 s, with the acceleration rate of 2000 rpm/s, using a 30 nm TiO_2 paste (Dyesol 30 NR-D) diluted in ethanol with 1 to 6 volume ratio. After the spin-coating, the substrates were dried at 80 ℃ for 10 min and then sintered at 450 ℃ for 30 min under dry air flow.

View Article Online
DOI: 10.1039/D1TA02878B

Perovskite layer

The perovskite precursor solution of $Cs_{0.1}FA_{0.9}Pb(I_{0.65}Br_{0.35})_3$ was prepared by dissolving a mixture of lead iodide (295.6 mg), lead bromide (260.11 mg), formamidinium iodide (208.98 mg), and cesium iodide (35.1 mg) in 1 mL mixture of DMF and DMSO (DMF (*v*):DMSO (*v*) = 4:1).

The perovskite solution of $Cs_{0.1}FA_{0.9}PbI_3$ was prepared by dissolving a mixture of lead iodide (622.35 mg), formamidinium iodide (208.98 mg) and cesium iodide (35.1 mg) in 1 mL mixure of DMF and DMSO (DMF (*v*):DMSO (*v*) = 4:1).

The perovskite solution was spin-coated through two-step program (1000 rpm for 10 s and 6000 rpm for 20 s) with pouring chlorobenzene as an anti-solvent 5s before the end of the second step. Then the substrates were annealed at 100 ℃ for 1 h in dry air.

Hole-transporting layer and Au contact

The substrates were cooled down to room temperature after annealing the perovskite. Spiro-MeOTAD solution was deposited by spin coating at 4000 rpm for 20 s as hole-transporting material. 90 mg spiro-MeOTAD was dissolved in 1 ml chlorobenzene, doped by 20.625 uL bis(trifluoromethylsulfonyl)imide lithium salt solution (520 mg/mL Li-TFSI in acetonitrile), and 35.5 uL 4-tert-Butylpyridine (TBP, Sigma-Aldrich). Finally, 80 nm of Au top electrode was deposited through thermal evaporator under high vacuum with an active area of 0.16 cm^2.

Simultaneous device and spectroscopic measurements

The devices were connected to a potentiostat (Biologic SP300), which was used to apply constant current or voltage and measure the voltage or current, respectively. Illumination was provided by a blue diode laser (422 nm, CW, Obis) and a diffuser to homogeneously illuminated the active area of a device, which was defined by an aperture. These illumination conditions are important to relate changes in PL with changes in current, voltage, and EL. Spectra have been recorded with a CCD spectrometer (Andor Kymera 193i with iDus DU240A-OE). Most devices have been measured under ambient conditions. The EL experiment taking several hours (Fig. 6) has been performed in a vacuum chamber. No qualitative differences between the two atmosphere conditions have been observed regarding light soaking. Only, EL experiments under vacuum lead to a slightly more stable signal when applying a constant current.